

Journal Pre-proof

Electrical characterization of basal cell carcinoma using a handheld electrical impedance dermography device

Xuesong Luo, Ye Zhou, Tristan Smart, Douglas Grossman, Benjamin Sanchez



PII: S2667-0267(21)00076-X

DOI: <https://doi.org/10.1016/j.xjidi.2021.100075>

Reference: XJIDI 100075

To appear in: *JID Innovations*

Received Date: 12 August 2021

Revised Date: 1 November 2021

Accepted Date: 2 November 2021

Please cite this article as: Luo X, Zhou Y, Smart T, Grossman D, Sanchez B, Electrical characterization of basal cell carcinoma using a handheld electrical impedance dermography device, *JID Innovations* (2021), doi: <https://doi.org/10.1016/j.xjidi.2021.100075>.

This is a PDF file of an article that has undergone enhancements after acceptance, such as the addition of a cover page and metadata, and formatting for readability, but it is not yet the definitive version of record. This version will undergo additional copyediting, typesetting and review before it is published in its final form, but we are providing this version to give early visibility of the article. Please note that, during the production process, errors may be discovered which could affect the content, and all legal disclaimers that apply to the journal pertain.

© 2021 Published by Elsevier Inc. on behalf of the Society for Investigative Dermatology.

**Electrical characterization of basal cell carcinoma using a handheld electrical impedance
dermography device**

Xuesong Luo¹, Ye Zhou¹, Tristan Smart³, Douglas Grossman^{2,3}, and Benjamin Sanchez¹

¹Department of Electrical and Computer Engineering, University of Utah, Salt Lake City, Utah.

²Department of Dermatology, University of Utah Health Sciences Center, Salt Lake City, Utah.

³Huntsman Cancer Institute, University of Utah Health Sciences Center, Salt Lake City, Utah.

Number of words in Abstract: 196

Number of words in manuscript: 3704

Number of figures: 5

Number of tables: 3

Number of supplementary figures: 1

Orcids: X Luo (0000-0003-4142-1402), Y Zhou (0000-0001-9367-7608), T Smart (0000-0002-0690-8736), D Grossman (0000-0003-1790-7023), B Sanchez (0000-0002-1594-9847)

Address correspondence to: Benjamin Sanchez, PhD, Sorenson Molecular Biotechnology Building, 36 S Wasatch Drive, Office 3721, Salt Lake City, UT 84112. Tel: 801-585-9535.

Email: benjamin.sanchez@utah.edu

Running title: Electrical characterization of BCC

ABSTRACT

Sensitive, objective, and easily applied methods for evaluating skin lesions are needed to improve diagnostic accuracy. In this study, we evaluated whether a developed noninvasive electrical impedance dermography (EID) device URSKIN could serve this purpose. In this pilot study, 17 subjects with subsequently confirmed basal cell carcinoma (BCC) underwent four-electrode EID measurements to assess the electrical properties of BCC and adjacent normal skin. A linear mixed-effects model with random intercept and slope terms was used for the analysis of multifrequency values in longitudinal and transverse directions. A significant difference in the intercept of frequency trajectories was observed for the longitudinal conductivity 0.13 S/m, $p < 0.001$, 95% confidence interval (CI) = 0.10 — 0.16; transverse conductivity 0.06 S/m, $p < 0.001$, 95% CI = 0.05 — 0.07; longitudinal relative permittivity (dimensionless) 203,742; $p < 0.001$, 95% CI = 180,292 — 227,191; and transverse relative permittivity (dimensionless) 86,894; $p < 0.001$, 95% CI = 81,549 — 92,238. Thus, our device detected significant electrical differences between BCC and adjacent normal skin. Given these preliminary performance metrics and its ease of use, this technology merits further study to establish its value in facilitating clinical diagnosis of skin cancers.

INTRODUCTION

While many skin cancers are easily recognized by the naked eye, they can be difficult to diagnose at early stages, and therefore there is a need and opportunity to develop technologies that can facilitate clinical diagnosis (March et al. 2015). Non-visual electrical impedance dermography (EID), a term coined by the authors to refer the specific application of impedance techniques for skin cancer assessment, is a technology based on detection of volume conduction differences between benign and malignant skin tissue (Braun et al. 2017; Rocha et al. 2017). These volume conduction properties (VCPs) reflect (1) how strongly skin resists or conducts alternating electrical current, and (2), its capacity to store electrical (positive and negative) ions charged inside and outside the cells. VCPs are uniquely determined by two physical electrical quantities: conductivity in International System of units of Siemens/meter (S/m) and relative permittivity (this is a dimensionless quantity as it is defined with respect to the permittivity of vacuum) (Foster and Schwan 1989). VCPs are characteristic physical properties (in the same way as the density, color, hardness, melting or boiling points) and represent an objective measure that describes the electrical status of the skin on a universally standard and absolute scale (Sanchez et al. 2021). Alterations in the internal composition and structure of cancerous skin tissue will result in an imbalance of the ionic content and cellular integrity, which will affect its VCPs.

To detect pathological changes inducing alterations in VCPs for skin diagnostic purposes, EID typically applies a low-intensity electrical alternating current to the tissue in a given area using two electrodes. As current flows through tissue, it generates a voltage signal that is then measured using the same (or different) electrodes. The voltage-to-current relationship determines the apparent electrical impedance of the skin (Stephens 1963), a quantity measured that arises

from the interaction of the skin conductivity and relative permittivity properties as well as their dependence with frequency of electrical current and direction of application (Yamamoto and Yamamoto 1976). Then, VCPs of skin can be inferred from impedance values using a biophysical model that describes the measurement configuration and the propagation of the electrical current within the skin.

Unlike the VCPs that are intrinsic characteristics of the skin, electrical impedance does not provide standardized values since they are also dependent on the electrode configuration (Geddes 1996). That is, simply by modifying the distance between the current and/or the voltage electrodes, the impedance values will be different even if the skin is exactly the same. Further, depending on the number of electrodes used to measure the skin, the impedance values will contain well as the contribution of the skin-electrode polarization impedance (Schwan 1992; McAdams et al. 1995) as it is the case for the Nevisense 2- and 3-electrode device (SciBase, Stockholm, Sweden). The skin-electrode polarization impedance arises from the interface between the electrode (a metallic conductor where the current charge carriers are electrons) and the body (where the electrical current conduction consists of the transit of ions, i.e., atoms of positive or negative charge). Importantly, the skin-electrode polarization impedance is a poorly controllable experimental factor where small alterations in skin-electrode contact area, skin humidity or temperature can give large impedance variations between measurements especially at low frequency (Alonso et al. 2020). While research has confirmed the diagnostic value of this approach (Glickman et al. 2003; Malvey et al. 2014), it still remains unknown to what extent impedance differences detected in those studies were solely generated by changes in the underlying VCPs in cancerous skin tissues and not a secondary interface effect between skin and the electrodes.

Here, we performed a pilot study testing a prototype of a 4-electrode EID device named URSKIN developed at the University of Utah for measuring in situ skin VCPs as well as their directionality. We determined the intrasession reproducibility of the technique, and assessed skin electrical differences between basal cell carcinoma (BCC) and adjacent normal skin.

Journal Pre-proof

RESULTS

Subject recruitment and lesion characteristics

A total of 18 subjects with skin lesions clinically suspicious for BCC were recruited for the study. Subject demographics and clinicopathologic characteristics of the lesions are detailed in Table 1. Given the intended use of the device for early detection of skin cancers, we targeted enrollment to early-stage lesions that were primarily macular and avoided larger palpable or ulcerated lesions. All lesions were assessed by a dermatologist (D.G.). Following EID measurements using URSKIN (Figure 1), all lesions were biopsied and 17/18 confirmed to be BCC. Eleven lesions exclusively revealed a superficial histologic pattern; five lesions revealed a combination of superficial, nodular, micronodular, and focally infiltrative patterns; and one lesion revealed a combination of micronodular and infiltrative patterns. One lesion (subject 12) revealed only telangiectasia, and was excluded from the analyses.

Device usability and reproducibility

A minimum of three impedance measurements at 6 different frequencies of electrical current ranging from 8 to 256 kiloHertz (kHz) were taken from lesional and adjacent clinically normal skin. The time required for data collection was less than 5 minutes per subject. Test-retest reproducibility data are summarized in Table 2. For both the lesional and normal skin measurements, intra-class correlation coefficient (ICC) conductivity values were lower at 8 and 16 kHz with mean values that ranged from 0.245 to 0.63. Comparatively, relative permittivity ICC values showed better reproducibility at 16 kHz with mean estimates from 0.673 to 0.822, where an ICC value of 1 represents a perfectly reproducible test. We found the most reproducible frequency range with highest ICC to be 128 kHz with mean estimates ranging from 0.61 to 0.913

except for longitudinal relative permittivity that was 32 kHz with ICC values 0.814 and 0.883 for lesional and normal skin, respectively.

Electrical differences between BCC and normal skin

Multi-frequency VCPs data including subject repeated measurements were analyzed and modeled with a mixed-effect linear model with random intercept and slope for BCC and normal skin, and the data are shown in Figure 2 and 3. Modeling a random slope gave lower Akaike scores compared to a random intercept model only both for conductivity and relative permittivity in longitudinal and transverse directions. We intentionally did not model the interaction between group and frequency because there is no physiological rationale supporting this dependence. For this, we included the slope in our linear effect model, which models the Maxwell-Wagner frequency-dependent relaxation due to cellular membrane permeability in the frequency range measured (Schwan 1984). As expected from the Maxwell-Wagner interfacial polarization mechanism in biological tissues, the slopes of both BCC and normal skin conductivity curves increase with frequency whereas the frequency dependence of relative permittivity curves is opposite. Modeling results, summarized in Table 3, reveal significant intercept differences ($p < 0.001$) between BCC and normal skin. These intercept differences are physiologically interpretable because they represent the VCPs of skin extrapolated at 0 Hz where the electric current flows only through the extracellular medium due to the capacitive behavior of cellular membranes. These results suggest the intercept is a sensitive model parameter to detect extracellular compositional and structural differences in BCC and adjacent non-lesional skin tissue.

DISCUSSION

The goal of this study was to evaluate the feasibility of our technology to measure the VCPs of BCC, the most common form of skin cancer. Thus, we focused our initial efforts on determining the reproducibility of the technique in a clinical setting and modeling differences between BCC and normal skin. The URSKIN device yielded highly reproducible measurements that revealed significant electrical differences between BCC and normal skin. Additionally, we found our device easy to use, and data collection was quick and painless for the subjects.

To assess the reproducibility, we performed repeated measurements with our electrode array placed over the skin lesion based on visual inspection. This somewhat imprecise approach to electrode placement may be offset to some extent by the fact that the array provides electrodes that are entirely fixed in position relative to one another, thus reducing intra-array differences in electrode spacing or orientation. Thus, the reproducibility of the electrode placement could be further improved by marking the skin with a marker or a pinpoint tattoo to assist in accurate placement during repeated measurements. Other potential sources of error affecting the reproducibility of the technique include the variability in the amount of saline used to moisten the skin prior to the measurements, the time to measurement after applying saline as well as the pressure applied to hold the electrode in place over the skin. Despite these potential confounding variables, the test-retest reproducibility was high at intermediate frequencies, suggesting that these frequencies could be potentially used to obtain reliable BCC measurements.

We used a mixed-effects linear model with random intercept and slope to understand lesional and normal skin conductivity and relative permittivity frequency-response trajectories. The use of multifrequency data in our modeling approach is based on the bioimpedance principle that has long recognized that single frequency data offer limited insight into tissue condition

(Grimnes and Martinsen 2014). Our modeled results indicate the ability to detect skin electrical changes associated with BCC versus adjacent normal skin. Histological alterations within developing BCC including scaling, telangiectasia, fibroplasia and other remodeling changes at the dermal-epidermal junction and in the dermis will likely impact the flow of electrical current through the lesion, supporting the observed differences in electrical conductivity and relative permittivity intercept values. Additional subject-specific factors that will likely affect our data that were not modeled here include age, gender, skin hydration status, extent of prior sun exposure and solar elastosis observed histologically, body site, skin temperature, and Fitzpatrick skin type and ethnicity. We suspect improvements will likely be achieved by accounting for these variables into our modeling approach which ultimately could impact accuracy of diagnosis.

In previous impedance studies on BCC (Beetner et al. 2003; Dua et al. 2004), electrical impedance readings were arbitrarily normalized via the calculation of a ratio between different frequencies in order to minimize skin-electrode impedance polarization artifacts and associated biological variations including body site, age and gender (Aberg et al. 2004, 2005). While this approach has shown clinical value for disease classification purposes, it has an important caveat: disentangling underlying physiological source(s) from ratiometric impedance values represents a technical complexity yet to overcome. For example, Birgersson et al. attempted to remove skin-electrode impedance polarization artifacts affecting SciBase II (Birgersson et al. 2013) but limitations associated with the approach resulted in large (up to 75%) skin VCP errors reported by the authors. As part of our impedance research efforts, we built a 4-electrode EID device robust to skin-electrode polarization errors and thus capable of measuring accurately VCPs of tissues and tested it in measurements on the tongue (Luo et al. 2020). The associated cost to obtain this information is an increase in measurement complexity since it required at least 12

electrodes to measure in at least 3 different directions (3 directions x 4 electrodes/direction) (Luo and Sanchez 2021). Here, we made changes to our system specifically for skin measurements including building a 16-electrode array. In total, 16 electrodes to measure in 4 different directions in order to have redundant data (4 directions x 4 electrodes/direction). Despite the increased complexity, the process of obtaining the VCPs of the skin with URSKIN is fully automated, transparent to the operator and required less than one minute to complete one skin measurement.

While URSKIN shows promise to improve cancer screening efficiency, further research is needed to assess its sensitivity and specificity for BCC diagnosis. The device is also limited in the number of frequencies and frequency range that it can measure, it may be possible to improve the sensitivity to detect alterations by increasing the number of frequencies, the frequency range measured as well as using an array of silicon nano- or micro-needles for penetrating the stratum corneum layer. However, these electrodes are not easy or cheap to manufacture and typically require access to a specialized silicon manufacturing facility. The design of the device must also balance minimizing invasiveness and maximizing reliability with durability and capability to completely penetrate the stratum corneum. Comparatively, widely-available printed circuit manufacturing processes used here provide a cost-efficient alternative making it relatively easy to make changes with a short lead time.

Additional computer simulations were performed to quantify the depth of skin measured with URSKIN, this information cannot be obtained through any other method. The simulation results indicate that the volume of tissue measured underneath the electrodes has dimensions of length 13 mm x width 17 mm x depth 7 mm (Figure 4). No differences in depth were observed between simulations changing the electrical current at the frequencies measured from 8 to 256

kHz. This depth sensitivity could be used to target the epidermis, papillary dermis, or reticular dermis simply by changing the spacing and arrangement of the electrodes. We foresee a future clinical translation of selective or spatial targeting to aid distinguishing superficial BCC from micronodular or infiltrative subtypes or determining sub-clinical extension of disease to guide therapy.

There are several limitations of this study. First, we intentionally did not address diagnostic differences in subjects with BCC versus healthy volunteers or compare skin VCPs with histological data, although all patients had histology performed as part of the study. Second, the technology employed was a custom-built prototype. For example, expanding the number of frequencies, the frequency range and the positioning of the current electrodes further from the voltage measuring electrodes would expect to allow us to fully characterize the VCPs of BCC and improve the sensitivity to detect even deeper skin lesions. Third, we modeled the VCPs of skin. Whereas prior work has demonstrated that various non-standardized relative impedance-derived metrics (e.g., arbitrarily defined ratios of impedance values at high and low frequencies) allow for BCC classification (Emtestam et al. 1998), values of electrical conductivity and relative permittivity in BCC reported here are, by definition, absolute (not relative) and standard. Clearly, the results will require further validation in future studies to evaluate different histologic subtypes of BCC, which we plan on pursuing as a logical next step to this work. Fourth, as a single site investigation, it will be important to replicate these findings in a multicenter cohort. Fifth, we have only examined a mixed-effects linear model in our outcomes. We are currently using machine learning approaches to obtain a more accurate representation of frequency trajectories including subject specific information and also to diagnose skin lesions. However, we are restricted from doing so here by the limited sample size in this pilot study.

Despite these limitations, we have shown that the technology we have developed provides a quick, convenient, reproducible means for performing EID in clinic of BCC and non-lesional adjacent skin. Our approach is noninvasive, provides objective, quantitative and standardized data reflecting the electrical status of the skin, its ease of use requires minimal operator training, and none of the subjects reported discomfort during the measurements. These early results suggest that our URSKIN is a promising biomarker for performing rapid and reliable skin lesion profiling in the clinical setting. Future studies generating normative lesional data, assessing the differences in electrical signature in other skin conditions, evaluating the utility in diagnosing skin cancer using machine learning approaches, and comparing skin electrical data with clinically accepted outcomes are planned.

MATERIALS & METHODS

Study subjects

This study was approved by the Institutional Review Board (IRB) at University of Utah and all participants gave prior written, informed consent. Our technology received IRB approval for human testing as a non-significant risk investigational device. A total of 18 patients were studied. The inclusion criteria were age 18 or older with a lesion clinically suspicious for BCC at least 5 mm in diameter that was to be biopsied. Subjects with lesions on the face, haired scalp, or genital area were excluded.

Experimental protocol

Figure 1 shows the device used in this study as well as the dimensions and details on the electrodes' disposition. The electrodes were sterilized with 70% isopropyl alcohol before each measurement. After informed written consent was obtained, any hairs around the lesion were removed using small scissors and the skin region cleaned using disposable gauze moistened with sterile saline. After 10 seconds, the electrode array was positioned against the skin applying gentle pressure to ensure good electrical contact. The operator then performed a measurement. The procedure was repeated at least two more times by the same operator to provide a minimum of three measurements. The device was taken off the skin in between repeated measurements and then positioned again. At the completion of the lesional measurements, a fresh piece of gauze was used to clean nearby normal skin at 2 inches from the lesion and the sequence repeated so that three or more control measurements were obtained. All measurements were obtained in approximately 5 minutes. As a part of standard of care, a shave biopsy of the suspicious lesion

was then performed and sent for routine processing and histologic analysis. The results of the biopsy, but not the EID measurements, were made available to the subjects.

Device

URSKIN is a portable handheld EID device to measure skin at the clinic. The device is powered by a battery and communicates with a custom smartphone app via Bluetooth (please see Supplementary Information and Figure S1 for further details regarding the use of the app). The device automatically applies a painless, safe, alternating electrical current starting at 8, 16, 32, 64, 128 and 256 kiloHertz (kHz) in four different directions sequentially as determined by the angles 0, 45, 90 and 150 degrees. To perform a measurement, the device automatically sweeps both the frequency of electrical current and the measuring direction sequentially. For each measuring direction (Figure 5), the device applies electrical current through outer ring current electrodes in that direction only (shown in red), and then measures the generated voltage through the inner voltage electrodes in that direction only (shown in blue).

The red arrow in Figure 5 is the electrical symbol for a current generator and the direction of the arrow indicates the direction of the current flow through the skin. As shown in Figure 5, the current generator applies alternating electrical current between the outer current electrodes. One of the current electrodes injects current into the skin while at the same time the opposite current electrode drains current from the skin needed to close the electrical circuit. At the same time, the inner voltage electrodes in that particular direction measure the generated electrical voltage. By measuring the difference between voltage electrodes using a voltmeter circuit and knowing the electrical current applied, the device calculates the skin impedance using Ohm's law: Impedance equals Voltage divided by Current. During a measurement, the current and

voltage electrodes in different directions from those colored in Figure 5B (i.e., electrodes shown in C, D, E); Figure 5C (i.e., electrodes shown in B, D, E); Figure 5D (i.e., electrodes shown in B, C, E); and Figure 5E (i.e., electrodes shown in B, C, D) are not connected to the current generator or the voltmeter and therefore not used.

Once the skin impedance data are measured in all four directions and frequencies, the device informs the operator via the smartphone app. At this point, the operator can remove the device from the skin since the measurement it is completed. At the same, the device automatically proceeds to process the data, this takes a few seconds only. Skin impedance data measured in all four directions at one specific frequency are processed by the device sequentially to calculate the skin conductivity and relative permittivity in longitudinal and transverse directions at that frequency in particular. Once the calculation is completed, the device proceeds to calculate the VCPs at the next frequency measured until all six measurement frequencies are analyzed. The result of these calculations are 24 different datasets: 2 (conductivity and relative permittivity) x 2 (longitudinal and transverse directions) x 6 (8, 16, 32, 64, 128, and 256 kHz). Next, the device transfers these data via Bluetooth to the app. Upon completion, the app notified the Operator and so that she/he can proceed to plot the data in the smartphone app to verify the values and perform a new measurement. De-identified data is automatically stored in the phone and also it can be sent from the app itself easily via email just by tapping the Send data button.

Electrode array

The skin electrode array is a custom designed printed circuit board manufactured by JLCPCB (Guangdong, China) (Figure 1). The printed circuit board contains a total of 16 noninvasive surface electrodes for 4-electrodes measurements defined by the angles 0, 45, 90 and 150

degrees. The outer pair of electrodes spaced 4.2 mm apart apply electrical current into the skin, whereas the inner pair electrodes at distance 2.8 mm apart measure the generated voltage signal.

Finite element model simulations

Finite element model (FEM) simulations were performed in the frequency domain using AC/DC Module, Electric Currents Physics in Comsol Multiphysics software, version 5.2 (Comsol, Inc., Burlington, Massachusetts). To determine the depth of measurement using URSKIN, we created a FEM rectangular slab mimicking a large portion of skin with dimensions 10 times larger than the electrodes' maximum distance as shown in Figure 1. The spatial dependence of the skin conductivity and relative permittivity properties were averaged from our clinically-normal measurements. The FEM was then broken down into small elements (a process termed discretization or meshing) from which to calculate individual element current and voltages shown in Figure 4. This computational process is necessary in order to quantitatively evaluate the depth of measurement via a numerical "sensitivity" analysis. This sensitivity analysis consists of quantifying the percentage contribution of each discretized element from the model to the impedance measured by the surface electrodes. The sensitivity region shown in Figure 4 reflects the overall expected skin volume measured with URSKIN contributing 99% out of a total of 100% to the measured data. In other words, cancer-induced electrical changes outside this colored sensitivity region are expected to contribute less than 1% to the recordings and they would probably be undetected with the simulated electrode configuration.

Data analysis

Skin conductivity and relative permittivity data were analyzed using R software (R Foundation for Statistical Computing, Viena, Austria). Standard intraclass correlation coefficients (ICCs) were calculated to describe how strongly repeated measurements resembled each other. ICCs are typically used to determine the technique's intrasession reproducibility as well as its 95% confidence intervals. Multi-frequency paired analysis was performed using a linear mixed-effects model for each dataset with random intercept and slope terms to account for within-subject correlations and between-subject variability. For these analyses, the main parameter of interest was the intercept difference since it has the most direct relevance to skin physiology.

DATA AVAILABILITY STATEMENT

Datasets related to this article can be found at the Sanchez Research Lab website at University of Utah (<https://srl.ece.utah.edu/publications/>).

CONFLICT OF INTEREST

Dr. Sanchez holds equity in Haystack Diagnostics, a company that develops clinical needle impedance technology for neuromuscular evaluation. The company has an option to license patented needle impedance technology where the author is named an inventor. He also holds equity and serves as Scientific Advisory Committee Member of Ioniq Sciences, a company that develops clinical impedance technology for early lung and breast cancer detection. Dr. Sanchez holds equity and serves as Scientific Advisor To The Board of B-Secur, a company that develops impedance technology. He consults for Myolex, Inc., a company that develops surface impedance technology. The company has an option to license patented surface impedance technology where the author is named an inventor. Dr. Sanchez also serves as a consultant to

Impedimed, a company that develops clinical impedance technology for early detection of secondary lymphedema. The company has an option to license patented impedance technology where the author is named an inventor. He also serves as a consultant to Texas Instruments, Happy Health, and Maxim Integrated, companies that develop impedance related technology for consumer use. Dr. Grossman is an investigator for Dermtech, Inc. and OrLucent, Inc., both companies developing non-invasive technologies for melanoma diagnosis, and also serves on the Advisory Board of OrLucent. The other authors have no conflicts to declare.

ACKNOWLEDGMENTS

D.G. was supported by the University of Utah Department of Dermatology and the Huntsman Cancer Foundation. The authors are thankful to Elise Brunsgaard and Dr. Kenneth Boucher, Co-Director of the Cancer Biostatistics Shared Resource at Huntsman Cancer Institute at the University of Utah, for their comments on the manuscript.

AUTHOR CONTRIBUTIONS

Developed the methods: X.L., B.S. Conceived and designed the experiments: D.G., B.S.

Performed the experiments: T.S. Analyzed the data: Y.Z., B.S., Wrote the paper: D.G., B.S. All authors reviewed and approved the final draft of the manuscript.

REFERENCES

- Aberg P, Geladi P, Nicander I, Hansson J, Holmgren U, Ollmar S. Non-invasive and microinvasive electrical impedance spectra of skin cancer - a comparison between two techniques. *Ski Res Technol*. 2005 Nov;11(4):281–6.
- Aberg P, Nicander I, Hansson J, Geladi P, Holmgren U, Ollmar S. Skin cancer identification using multifrequency electrical impedance--a potential screening tool. *IEEE Trans Biomed Eng*. 2004 Dec;51(12):2097–102.
- Alonso E, Giannetti R, Rodríguez-Morcillo C, Matanza J, Muñoz-Frías JD. A Novel Passive Method for the Assessment of Skin-Electrode Contact Impedance in Intraoperative Neurophysiological Monitoring Systems. *Sci Rep*. 2020 Dec 18;10(1):2819.
- Beetner DG, Kapoor S, Manjunath S, Zhou X, Stoecker W V. Differentiation among basal cell carcinoma, benign lesions, and normal skin using electric impedance. *IEEE Trans Biomed Eng*. 2003 Aug;50(8):1020–5.
- Birgersson U, Birgersson E, Nicander I, Ollmar S. A methodology for extracting the electrical properties of human skin. *Physiol Meas*. 2013 Jun;34(6):723–36.
- Braun RP, Mangana J, Goldinger S, French L, Dummer R, Marghoob AA. Electrical Impedance Spectroscopy in Skin Cancer Diagnosis. *Dermatol Clin*. 2017 Oct;35(4):489–93.
- Dua R, Beetner DG, Stoecker W V, Wunsch DC. Detection of basal cell carcinoma using electrical impedance and neural networks. *IEEE Trans Biomed Eng*. 2004 Jan;51(1):66–71.
- Emtestam L, Nicander I, Stenström M, Ollmar S. Electrical impedance of nodular basal cell carcinoma: a pilot study. *Dermatology*. 1998;197(4):313–6.
- Foster KR, Schwan HP. Dielectric properties of tissues and biological materials: a critical review. *Crit Rev Biomed Eng*. 1989;17(1):25–104.

- Geddes LA. Who introduced the tetrapolar method for measuring resistance and impedance?
IEEE Eng Med Biol Mag. 1996;15(5):133–4.
- Glickman YA, Filo O, David M, Yayon A, Topaz M, Zamir B, et al. Electrical impedance scanning: a new approach to skin cancer diagnosis. *Ski Res Technol*. 2003 Aug;9(3):262–8.
- Grimnes S, Martinsen OG. *Bioimpedance and Bioelectricity Basics*. 3rd ed. Academic Press; 2014.
- Luo X, Gutierrez Pulido HV, Rutkove SB, Sanchez B. In vivo muscle conduction study of the tongue using a multi-electrode tongue depressor. *Clin Neurophysiol*. 2020 Dec;20(30555–1):S1388-2457.
- Luo X, Sanchez B. In silico muscle volume conduction study validates in vivo measurement of tongue volume conduction properties using the UTA depressor. *Physiol Meas*. 2021;42(4):045009.
- Malvey J, Hauschild A, Curiel-Lewandrowski C, Mohr P, Hofmann-Wellenhof R, Motley R, et al. Clinical performance of the Nevisense system in cutaneous melanoma detection: an international, multicentre, prospective and blinded clinical trial on efficacy and safety. *Br J Dermatol*. 2014 Nov;171(5):1099–107.
- March J, Hand M, Grossman D. Practical application of new technologies for melanoma diagnosis. *J Am Acad Dermatol*. 2015 Jun;72(6):929–41.
- McAdams ET, Lackermeier A, McLaughlin JA, Macken D, Jossinet J. The linear and non-linear electrical properties of the electrode-electrolyte interface. *Biosens Bioelectron*. 1995 Jan;10(1–2):67–74.
- Rocha L, Menzies SW, Lo S, Avramidis M, Khoury R, Jakkett L, et al. Analysis of an electrical impedance spectroscopy system in short-term digital dermoscopy imaging of melanocytic

lesions. *Br J Dermatol.* 2017 Nov 11;177(5):1432–8.

Sanchez B, Martinsen OG, Freeborn TJ, Furse CM. Electrical impedance myography: A critical review and outlook. *Clin Neurophysiol.* 2021 Feb;132(2):338–44.

Schwan HP. Electrical and acoustic properties of biological materials and biomedical applications. *IEEE Trans Biomed Eng.* 1984 Dec;31(12):872–8.

Schwan HP. Linear and nonlinear electrode polarization and biological materials. *Ann Biomed Eng.* 1992 May;20(3):269–88.

Stephens WGS. The current-voltage relationship in human skin. *Med Electron Biol Eng.* 1963 Aug;1(3):389–99.

Yamamoto T, Yamamoto Y. Electrical properties of the epidermal stratum corneum. *Med Biol Eng.* 1976 Mar;14(2):151–8.

TABLES

Table 1. Subject demographics and clinicopathologic features of lesions.

Subject #	Age	Sex (M,F)	Body site	Lesion size (mm)	Diagnosis	BCC subtype
1	63	M	Shoulder	5	BCC	Superficial
2	73	M	Shoulder	5	BCC	Superficial
3	91	F	Arm	10	BCC	Superficial, focally Infiltrative
4	36	F	Forearm	5	BCC	Superficial, micronodular
5	74	M	Clavicle	6	BCC	Superficial, nodular
6	76	F	Forearm	6	BCC	Superficial
7	59	M	Back	5	BCC	Superficial, nodular
8	52	M	Back	5	BCC	Superficial
9	44	M	Scalp	7	BCC	Superficial, nodular
10	54	M	Back	7	BCC	Superficial
11	58	M	Shoulder	7	BCC	Superficial
12 (excluded)	49	F	Hand	5	Telangiectasia	N/A
13	55	M	Back	11	BCC	Superficial
14	73	F	Arm	6	BCC	Superficial
15	60	M	Neck	7	BCC	Superficial
16	48	F	Back	9	BCC	Superficial
17	35	F	Shoulder	6	BCC	Micronodular, infiltrative
18	61	F	Shin	6	BCC	Superficial

Table 2. Summary of test versus retest reproducibility for multi-frequency conductivity and relative permittivity values. Estimates of intra-class correlation coefficients and 95% confidence intervals.

Frequency (kHz)		<i>Longitudinal conductivity</i>		<i>Transverse conductivity</i>		<i>Longitudinal relative permittivity</i>		<i>Transverse relative permittivity</i>	
		<i>Estimates</i>	<i>Conf. Int. (95%)</i>	<i>Estimates</i>	<i>Conf. Int. (95%)</i>	<i>Estimates</i>	<i>Conf. Int. (95%)</i>	<i>Estimates</i>	<i>Conf. Int. (95%)</i>
8	BCC	0.334	0.034 - 0.65	0.445	0.146 - 0.72	0.379	0.087 - 0.673	0.548	0.227 - 0.76
	Normal	0.245	-0.053 - 0.586	0.3	0.011 - 0.622	0.595	0.308 - 0.816	0.494	0.203 - 0.755
16	BCC	0.384	0.079 - 0.686	0.63	0.352 - 0.835	0.731	0.502 - 0.885	0.739	0.435 - 0.889
	Normal	0.258	-0.059 - 0.611	0.478	0.173 - 0.753	0.673	0.405 - 0.862	0.822	0.64 - 0.93
32	BCC	0.545	0.234 - 0.801	0.0569	-0.23 - 0.457	0.814	0.615 - 0.9	0.645	0.257 - 0.858
	Normal	0.247	-0.038 - 0.589	0.709	0.462 - 0.878	0.883	0.745 - 0.955	0.869	0.726 - 0.949
64	BCC	0.775	0.562 - 0.909	0.776	0.563 - 0.91	0.713	0.467 - 0.88	0.481	0.107 - 0.742
	Normal	0.58	0.272 - 0.821	0.62	0.323 - 0.841	0.275	-0.028 - 0.625	0.704	0.432 - 0.882
128	BCC	0.715	0.122 - 0.715	0.832	0.667 - 0.931	0.00571	-0.236 - 0.347	0.728	0.44 - 0.88
	Normal	0.843	0.683 - 0.936	0.61	0.328 - 0.824	0.449	0.147 - 0.729	0.913	0.816 - 0.966
256	BCC	0.535	0.238 - 0.787	0.822	0.631 - 0.93	0.225	-0.072 - 0.579	0.656	0.264 - 0.861
	Normal	0.29	-0.006 - 0.624	0.523	0.213 - 0.7-82	0.111	-0.18 - 0.491	0.605	0.317 - 0.826

Table 3. Summary of modeled conductivity and relative permittivity differences. Estimates, 95% confidence intervals and statistical significance p -values obtained analyzing multi-frequency values using a linear mixed-effects model for each dataset with random intercept and slope terms.

Predictors	Longitudinal conductivity			Transverse conductivity			Longitudinal relative permittivity			Transverse relative permittivity		
	Estimates	Conf. Int. (95%)	P-Value	Estimates	Conf. Int. (95%)	P-Value	Estimates	Conf. Int. (95%)	P-Value	Estimates	Conf. Int. (95%)	P-Value
Intercept	129.84 E-3	100.6 7E- 3 – 159.0 1E-3	<0.001	59.35 E-3	52.17E - 3 – 66. 53E-3	<0.001	203742 .03	180292.5 8 – 2271 91.49	<0.001	86895. 27	81554.2 5 – 92236 .29	<0.001
Frequency	1.5E-3	1.25E -3 – 1.74E -3	<0.001	0.25E -3	0.21E- 3 – 0.3 0E-3	<0.001	-892.74	-1055.21 – -730.28	<0.001	-401.59	-441.78 – -361.41	<0.001

FIGURE LEGENDS

Figure 1. Handheld electrical impedance dermography (EID) device tested in this study.

(A) Use example in the clinic. (B) The reduced dimensions and portability of URSKIN allow the operator to hold the device with one hand while with the other hand controls the device with a smartphone (Please see Supplementary Information for additional details). (C) The electrode spacing used here constrains the minimum lesion size to 5 mm.

Figure 2. Conductivity of basal cell carcinoma and normal adjacent skin. BCC (red) and non-lesional adjacent skin (blue) dots represent individual conductivity values obtained in (A) longitudinal and (B) transverse directions including all repeated measurements and subjects. The solid lines are the modeled trajectories including 95% confidence intervals.

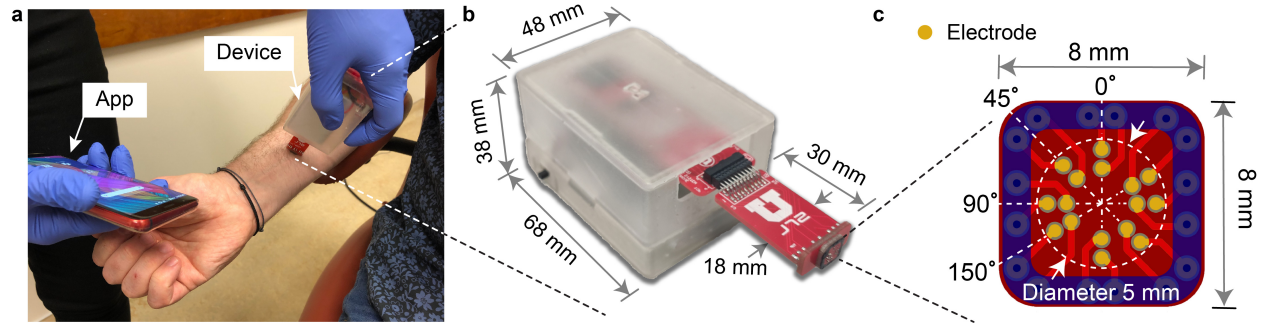
Figure 3. Relative permittivity of basal cell carcinoma and normal adjacent skin. BCC (red) and non-lesional adjacent skin (blue) dots represent individual relative permittivity values obtained in (A) longitudinal and (B) transverse directions including all repeated measurements and subjects. The solid lines are the modeled trajectories including 95% confidence intervals.

Figure 4. Electrical impedance dermography (EID) simulation. (A) Qualitative finite element model (FEM) simulation at 8 kHz shows the distribution of electrical current through the skin model and the voltage surfaces generated within the tissue during an EID measurement. (B) Quantitative FEM analysis to assess the region of tissue and depth underlying the electrodes measured with URSKIN.

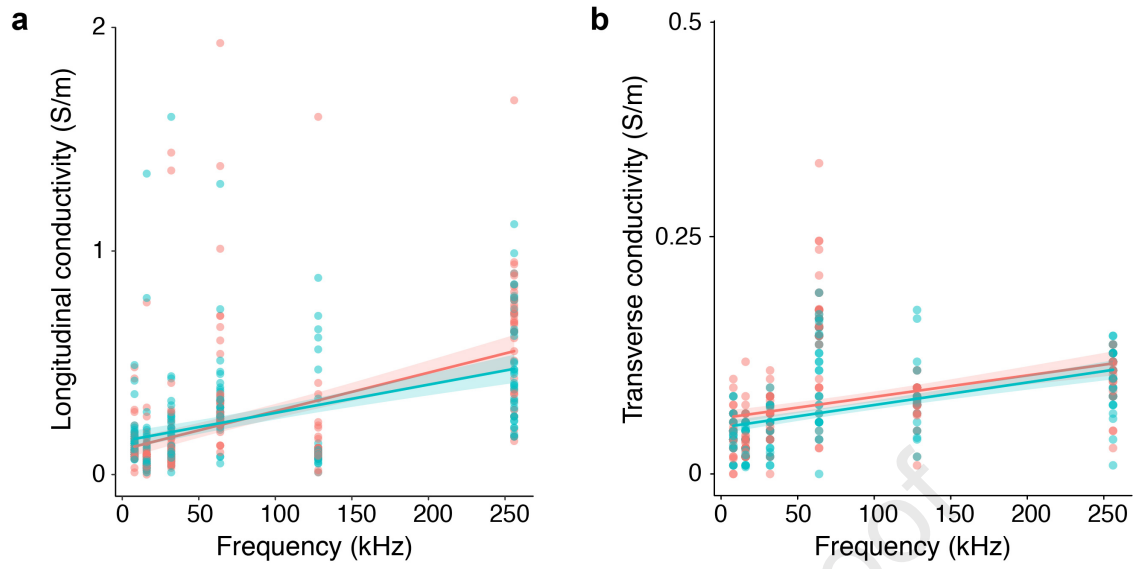
Figure 5. Electrical connections to perform an electrical impedance dermography (EID) measurement. (A) Schematic illustrating a plan view of the 16-electrode array. Electrical connection of the current generator and voltmeter to the outer current (in red) and inner voltage (in blue) electrodes measuring in 4 directions: (B) 0, (C) 45, (D), 90, (E) 150 degrees.

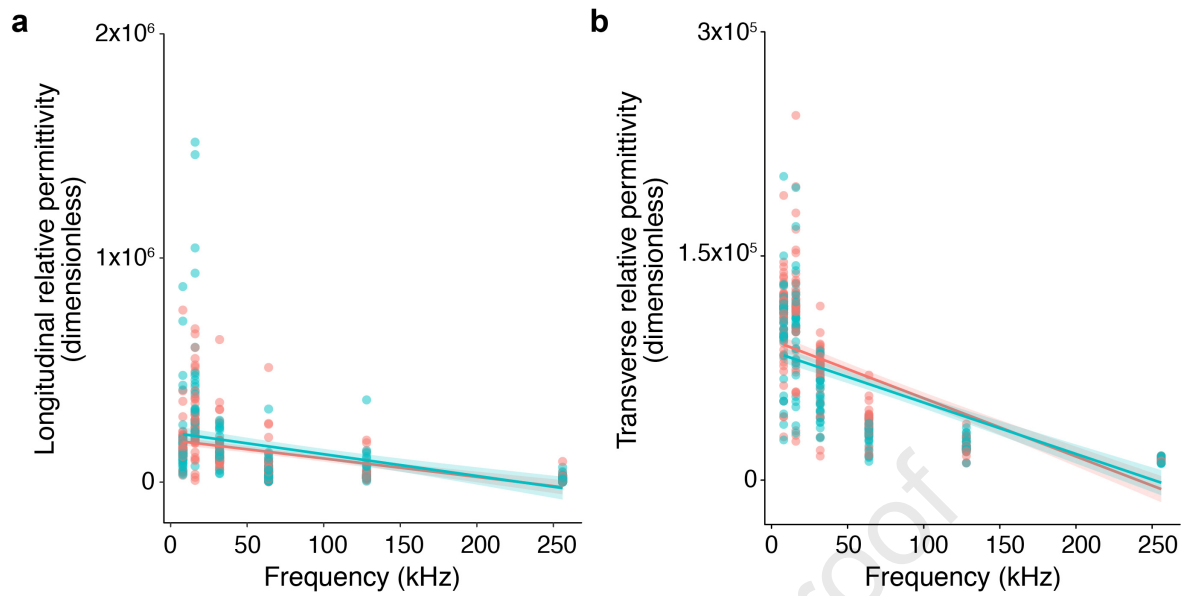
Supplementary Figure 1. App user interface. The app guides the operator from step A to J to complete a measurement and email the data for further analysis.

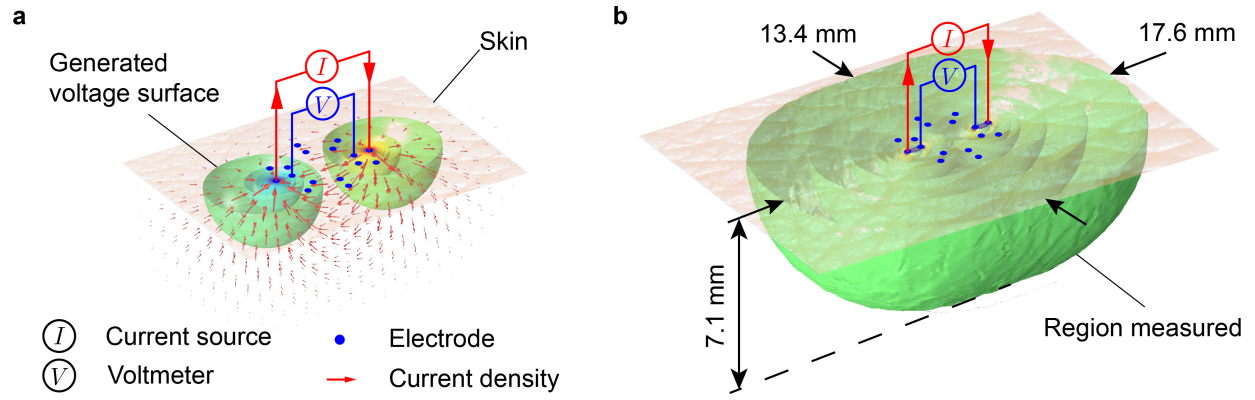
Journal Pre-proof

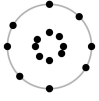
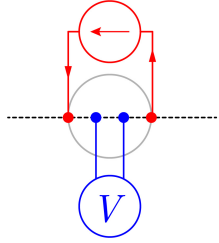
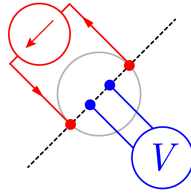
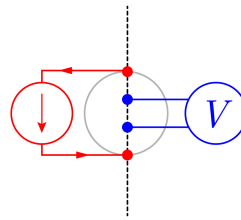
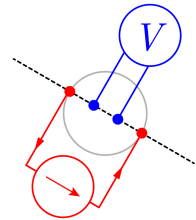


Journal Pre-proof







a 16-electrode skin array**b** 0 deg**c** 45 deg**d** 90 deg**e** 150 deg

Journal Pre-proof